Molecular Therapy
Nucleic Acids
Original Article

A peptide inhibitor that rescues polyglutamine-induced synaptic defects and cell death through suppressing RNA and protein toxicities

Shaohong Isaac Peng,[1] Lok I. Leong,[1] Jacquelyne Ka-Li Sun,[1] Zhefan Stephen Chen,[1] Hei-Man Chow,[1,2] and Ho Yin Edwin Chan[1,2,3]

[1]School of Life Sciences, The Chinese University of Hong Kong, Shatin N.T., Hong Kong SAR, China; [2]Nexus of Rare Neurodegenerative Diseases, The Chinese University of Hong Kong, Shatin N.T., Hong Kong SAR, China; [3]Gerald Choa Neuroscience Centre, The Chinese University of Hong Kong, Shatin N.T., Hong Kong SAR, China

Polyglutamine (polyQ) diseases, including spinocerebellar ataxias and Huntington's disease, are progressive neurodegenerative disorders caused by CAG triplet-repeat expansion in the coding regions of disease-associated genes. In this study, we found that neurotoxic small CAG (sCAG) RNA species, microscopic Ataxin-2 CAG RNA foci, and protein aggregates exist as independent entities in cells. Synaptic defects and neurite outgrowth abnormalities were observed in mutant Ataxin-2-expressing mouse primary cortical neurons. We examined the suppression effects of the CAG RNA-binding peptide beta-structured inhibitor for neurodegenerative diseases (BIND) in mutant Ataxin-2-expressing mouse primary cortical neurons and found that both impaired synaptic phenotypes and neurite outgrowth defects were rescued. We further demonstrated that BIND rescued cell death through inhibiting sCAG RNA production, Ataxin-2 CAG RNA foci formation, and mutant Ataxin-2 protein translation. Interestingly, when the expanded CAG repeats in the mutant Ataxin-2 transcript was interrupted with the alternative glutamine codon CAA, BIND's inhibitory effect on mutant protein aggregation was lost. We previously demonstrated that BIND interacts physically and directly with expanded CAG RNA sequences. Our data provide evidence that the BIND peptide associates with transcribed mutant CAG RNA to inhibit the formation of toxic species, including sCAG RNA, RNA foci, and polyQ protein translation and aggregation.

INTRODUCTION

Polyglutamine (polyQ) diseases, including Huntington's disease and several types of spinocerebellar ataxias (SCAs), are progressive neurodegenerative disorders caused by genomic CAG triplet-repeat expansion. PolyQ toxicity is mediated through the transcription of expanded CAG repeats in the exons of disease-associated genes, including *huntingtin* and *ataxins*. Transcripts carrying mutant CAG repeats produce proteins containing elongated polyQ stretches.[1] Overexpression of polyQ protein in mice leads to polyQ protein aggregate formation and progressive neurological defects.[2] Sequestration of soluble proteins into polyQ aggregates leads to deficits in cellular functions. For instance, sequestration of the CREB-binding protein (CBP), a transcription regulator, into polyQ protein aggregates results in a reduction in the soluble CBP level and downregulation of CBP-mediated gene transcription.[3] Ceasing the expression of the mutant polyQ transgene in symptomatic mice can result in the clearance of polyQ aggregates and the reversal of locomotor abnormalities.[4] These findings highlight the involvement of polyQ protein aggregates in disease pathogenesis. Besides protein aggregation, expanded CAG RNAs are capable of forming RNA foci.[5] When mutant expanded triplet CAG-repeat sequences are inserted into the untranslated region of a reporter construct, the transcribed elongated CAG RNA no longer produces the polyQ protein. Under this condition, neurodegeneration has been detected in animal models.[6] This finding suggests that non-translatable elongated CAG RNA can still elicit neurotoxicity. This phenomenon is termed CAG RNA toxicity. Expanded CAG-repeat-containing transcripts can serve as substrates of Dicer to produce small CAG RNA species,[7] triggering the silencing of CUG-containing RNAs in polyQ disease models[8] and patients.[9] We previously reported that the sCAG RNA-mediated gene-silencing mechanism causes the downregulation of *NUDT16* expression, which results in the induction of cellular DNA damage.[10] The genomic expansion of CAG repeats causes the transcription of mutant CAG transcripts, which further leads to the production of sCAG RNA and the formation of RNA foci and polyQ protein aggregates. These species all contribute to the pathogenesis of polyQ disease.

Our group has developed peptide inhibitors to neutralize CAG RNA toxicity in polyQ degeneration.[11,12] The design of these inhibitors was based on the nucleolin (NCL) protein.[13] The NCL protein carries four RNA recognition motifs (RRMs). We previously reported that the NCL RRM2 and RRM3 domains directly interact with CAG RNA.[14] The 21 amino acid peptide **b**eta-structured **i**nhibitor for

Received 7 December 2021; accepted 7 June 2022;
https://doi.org/10.1016/j.omtn.2022.06.004.

Correspondence: Ho Yin Edwin Chan, School of Life Sciences, The Chinese University of Hong Kong, Shatin N.T., Hong Kong SAR, China.
E-mail: hyechan@cuhk.edu.hk

neurodegenerative **d**iseases (BIND) interacts with expanded CAG RNA at low micromolar levels.[12] This peptide is also capable of rescuing cell death in mutant CAG RNA-expressing cells.[12]

In this study, we examined sCAG production, RNA foci formation, and polyQ protein translation and aggregation in an Ataxin-2 disease cell model and showed that mutant Ataxin-2 cytotoxicity positively correlated with the abundance of these toxic species in both a CAG-repeat-length- and time-dependent manner. Treating Ataxin-2-expressing cells with the peptide inhibitor BIND led to a significant reduction in all of the above biomarkers, including the sCAG level, RNA foci, polyQ translation and aggregation, and cell death. BIND treatment also rescued mutant Ataxin-2-induced synaptic defects in mouse primary cortical neurons.

RESULTS

Mutant expanded CAG RNA induces cytotoxicity by contributing to sCAG RNA production, RNA foci formation, and polyQ protein aggregation

To investigate different neurotoxic species in Ataxin-2 pathologies, mutant Ataxin-2 constructs containing ascending numbers of CAG repeats ($SCA2_{CAG22/42/72/104}$) were expressed in SK-N-MC neuroblastoma cells. We recently reported that sCAG RNAs, which are cleaved from expanded CAG-repeat transcripts by the ribonuclease Dicer,[15] cause silencing of *NUDT16* and trigger genomic DNA damage.[10] Here, we observed robust sCAG RNA production in $SCA2_{CAG42/72/104}$-expressing cells. The increasing amounts of sCAG RNAs were positively correlated with the CAG-repeat lengths of the constructs (Figure 1A). As previously reported, the generation of toxic sCAG RNAs resulted in silencing of *NUDT16* in these cells, lowering the level of *NUDT16* transcription and NUDT16 protein expression (Figure 1A). We also found that this subsequently led to the phosphorylation of ATR/checkpoint kinase 1 (CHK1) and ATM/CHK2 (Figure 1A), indicating the activation of both the single- and double-stranded DNA-damage-response signaling pathways.[16,17] We further detected an enhanced level of caspase 3 cleavage (Figure 1A), which is a marker of cell death. In contrast, the levels of sCAG RNA, NUDT16, phosphorylated DNA-damage-related kinases, and cleaved caspase 3 in the unexpanded $SCA2_{CAG22}$-expressing cells remained similar to those in the untransfected control cells (Figure 1A). Moreover, knock down of Dicer was found to suppress the activation of the above DNA damage kinases and the cleavage of caspase 3, illustrating the role of Dicer in cleaving the expanded CAG RNAs into the sCAG RNAs that led to cellular DNA damage and apoptosis (Figure S1). A comet assay was then performed to measure the tail moment of damaged DNA migrating away from the nucleus, which indicates the amount of DNA breakage.[18] Significant DNA damage was not observed in $SCA2_{CAG22}$-expressing cells when compared with the untransfected control. In $SCA2_{CAG42/72/104}$-transfected cells, higher levels of DNA damage were induced in a CAG-repeat-length-dependent manner (Figures 1B and 1C).

Aside from being cleaved into toxic sCAG RNAs, mutant expanded CAG RNA forms RNA foci and/or is translated into aggregation-prone expanded polyQ protein. Both CAG RNA foci and polyQ protein aggregates are signature pathogenic hallmarks of polyQ diseases.[19,20] Expanded CAG RNA foci are involved in some gain-of-function and cellular protein sequestration pathological mechanisms that confer neuronal RNA toxicity.[21] Expanded polyQ protein tracts are prone to misfolding to form monomers, oligomers, insoluble aggregates with amyloid fibrils, and intracellular inclusions that contribute to neuronal protein toxicity.[20,22] We next conducted a fluorescence *in situ* hybridization (FISH) assay to detect CAG RNA foci formation and polyQ protein aggregation in the Ataxin-2 cell models. In cells expressing $SCA2_{CAG42/72/104}$, elevated levels of CAG RNA foci (Figures 1D and 1E) and polyQ aggregates (Figures 1D and 1F) were detected, and the extent of the RNA foci and polyQ aggregates was positively correlated with the CAG-repeat lengths of the Ataxin-2 constructs. A filter-trap assay was performed to demonstrate that the extent of insoluble polyQ aggregation increased in line with the increasing CAG-repeat number of the constructs (Figure 1G). In the unexpanded control $SCA2_{CAG22}$-transfected cells, no significant CAG RNA foci formation nor polyQ protein aggregation was observed (Figures 1D–1G). Taken together, these results revealed that expanded CAG RNA was the culprit in generating multiple neurotoxic molecules, including sCAG RNAs, CAG RNA foci, and polyQ protein aggregates, all of which contribute to overall cytotoxicity (Figure 1H).

We further observed that the extent of cellular DNA damage (Figures S2A–S2C), RNA foci formation (Figures S2D and S2E), protein aggregation (Figures S2D, S2F, and S2G), and subsequent cell death (Figure S2H) progressed in a time-dependent manner from 24 to 48/72 h. In contrast, these markers in the unexpanded $SCA2_{CAG22}$ controls remained at comparable levels to those in the untransfected controls throughout the incubation period (Figure S2). Our findings highlight that the CAG-repeat-length- and progressive time dependency of sCAG RNA production, CAG RNA foci formation, and polyQ protein aggregation plays an important role in polyQ pathogenesis.

sCAG RNA, CAG RNA foci, and polyQ protein aggregates individually contribute to mutant Ataxin-2 cytotoxicity

We generated two mutant Ataxin-2 constructs, $SCA2^{\Delta ATG}{}_{CAG115}$ and $SCA2_{CAA/G104}$, to examine the independent contribution of sCAG RNA, RNA foci, and protein aggregation to mutant Ataxin-2 cytotoxicity. The $SCA2^{\Delta ATG}{}_{CAG115}$ construct lacks the ATG initiation codon, while the $SCA2_{CAA/G104}$ construct carries non-continuous CAG repeats. We showed that $SCA2^{\Delta ATG}{}_{CAG115}$–expressing cells displayed sCAG RNA (Figure 2A) and CAG RNA foci (Figures 2D and 2E) but not polyQ protein translation (Figure 2B) nor aggregation (Figures 2C, 2D, and 2F). On the contrary, $SCA2_{CAA/G104}$–expressing cells only displayed polyQ protein (Figure 2B) and aggregates (Figures 2C, 2D, and 2F) but not sCAG RNA (Figure 2A) and CAG RNA foci (Figures 2D and 2E). Importantly, only a moderate level of cell death was observed in either the sCAG RNA-/RNA foci-presenting $SCA2^{\Delta ATG}{}_{CAG115}$ cells or polyQ protein-/aggregate-presenting $SCA2_{CAA/G104}$ cell model (Figure 2G) when compared with those that were transfected with the unmodified $SCA2_{CAG104}$ model

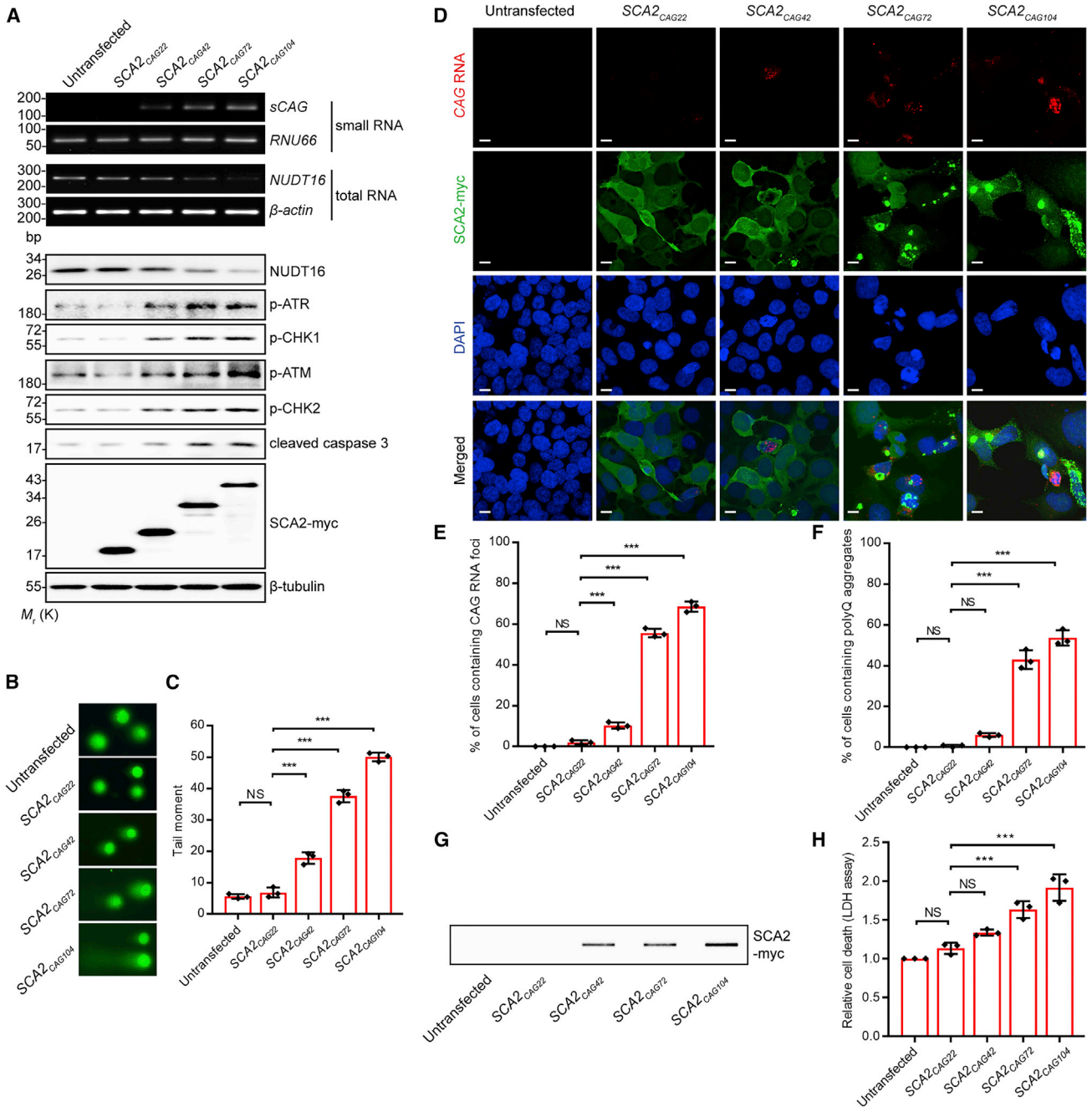

Figure 1. The generation of small CAG RNA, CAG RNA foci, and polyQ protein aggregates are positively correlated with the CAG repeats of the Ataxin-2 constructs

(A) Elevated levels of small CAG (*sCAG*) RNA, phosphorylated ATR (p-ATR), CHK1 (p-CHK1), ATM (p-ATM), CHK2 (p-CHK2), and cleaved caspase 3 proteins were detected in $SCA2_{CAG42/72/104}$-expressing SK-N-MC cells. Both the NUDT16 mRNA and protein levels were reduced. (B) Increased DNA damage was observed in the SK-N-MC cells transfected with $SCA2_{CAG42/72/104}$ constructs. (C) Quantification of (B). (D) The frequency of CAG RNA foci and polyQ protein aggregates increased with CAG repeats in $SCA2_{CAG42/72/104}$-expressing cells. Scale bars: 10 μm. (E and F) Quantification of (D). (G) Filter-trap analysis showed an increase in SDS-insoluble Ataxin-2 protein in $SCA2_{CAG42/72/104}$-expressing SK-N-MC cells. (H) Increased level of cell death was detected in $SCA2_{CAG42/72/104}$-expressing SK-N-MC cells. Error bars represent ± SD. Statistical analysis was performed using one-way ANOVA. NS indicates no significance, ***$p < 0.001$. *RNU66*, *beta-actin*, and beta-tubulin were used as loading controls. Experiments were independently repeated for three times. Only representative images, gels, and blots are shown.

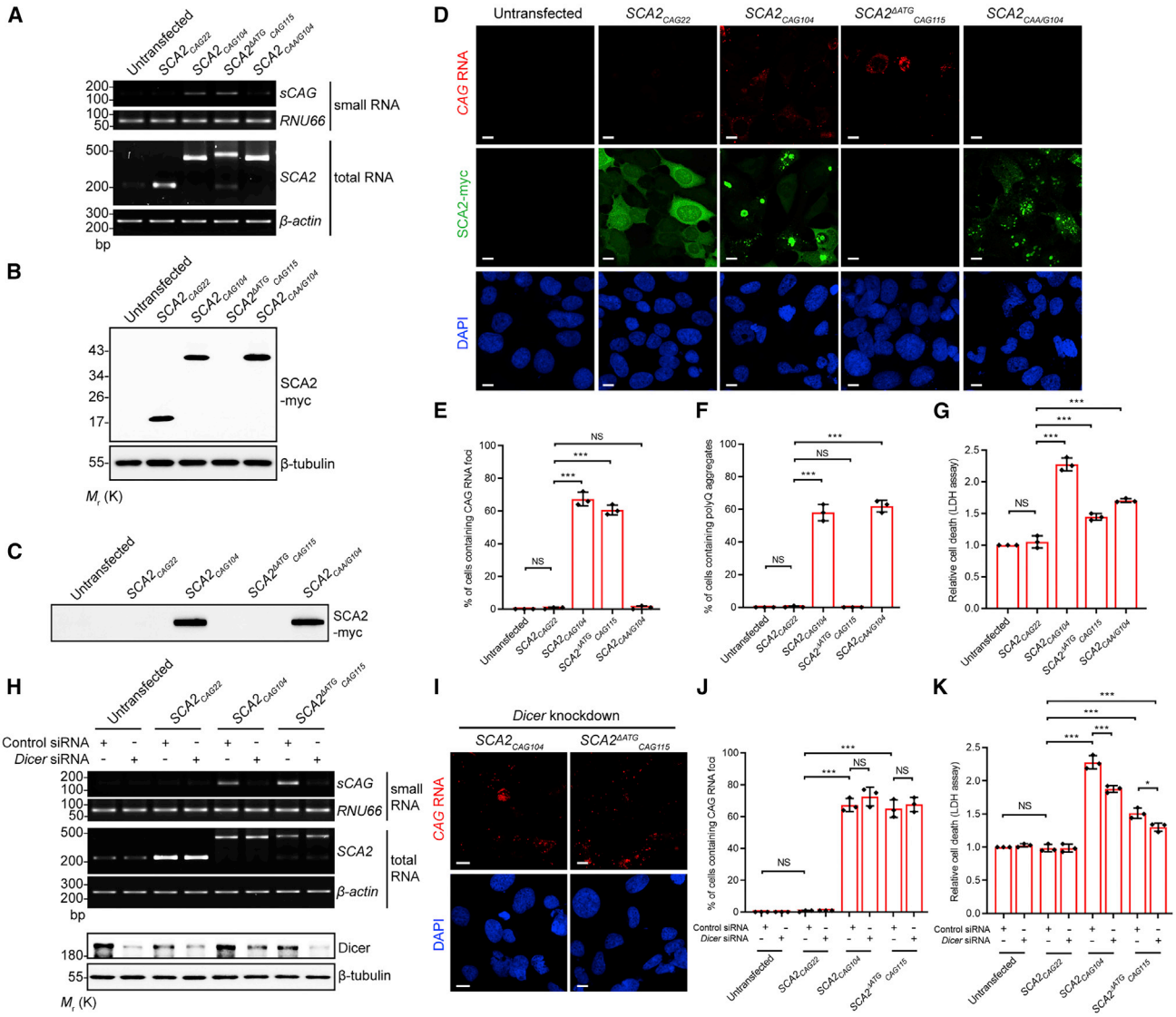

Figure 2. Both expanded CAG RNA and polyQ protein aggregates contribute to mutant Ataxin-2 cytotoxicity

(A) Elevated levels of *sCAG* RNA were detected in SK-N-MC cells transfected with $SCA2_{CAG104}$ or $SCA2^{\Delta ATG}_{CAG115}$ (RNA toxicity) but not in cells expressing $SCA2_{CAA/G104}$ (protein toxicity). (B) polyQ protein translation was observed in $SCA2_{CAG104}$- or $SCA2_{CAA/G104}$-expressing SK-N-MC cells but not in $SCA2^{\Delta ATG}_{CAG115}$-expressing cells. (C) Filter-trap result showed increased level of SDS-insoluble mutant Ataxin-2 protein in SK-N-MC cells expressing $SCA2_{CAG104}$ or $SCA2_{CAA/G104}$. (D) SK-N-MC cells transfected with $SCA2_{CAG104}$ displayed both CAG RNA foci and polyQ protein aggregates. $SCA2^{\Delta ATG}_{CAG115}$-expressing cells displayed only CAG RNA foci formation but not polyQ protein aggregation. Only polyQ protein aggregates were observed in $SCA2_{CAA/G104}$-expressing cells. Scale bars: 10 μm. (E and F) Quantification of (D). (G) Moderate level of cell death was observed in SK-N-MC cells transfected with either $SCA2^{\Delta ATG}_{CAG115}$ or $SCA2_{CAA/G104}$ when compared with cells expressing $SCA2_{CAG104}$. (H) sCAG RNA production was suppressed upon the knock down of Dicer in both $SCA2_{CAG104}$- and $SCA2^{\Delta ATG}_{CAG115}$-expressing SK-N-MC cells. (I) Knocking down Dicer expression did not alter CAG RNA foci formation in $SCA2_{CAG104}$- and $SCA2^{\Delta ATG}_{CAG115}$-expressing SK-N-MC cells. (J) Quantification of (I). (K) Cell death induced by $SCA2_{CAG104}$ and $SCA2^{\Delta ATG}_{CAG115}$ was partially rescued upon the knock down of Dicer. Error bars represent ± SD. Statistical analysis was performed using one-way ANOVA. NS indicates no significance, *p < 0.05, ***p < 0.001. *RNU66*, *beta-actin*, and beta-tubulin were used as loading controls. Experiments were independently repeated for three times. Only representative images, gels, and blots are shown.

(Figure 2G). This indicates that both CAG RNA and polyQ protein species can individually induce cytotoxicity.

The transcription of mutant Ataxin-2 construct generates sCAG RNA (Figure 1A) and RNA foci (Figure 1D). Dicer is crucial for sCAG RNA production.[7] We examined the abundance of sCAG RNA and CAG RNA foci in $SCA2_{CAG104}$-expressing cells under both control and Dicer-knockdown conditions and found that Dicer knockdown only abolished sCAG RNA production (Figure 2H) and did not exert any effect on CAG RNA foci formation (Figures 2I and 2J). We next

examined whether Dicer knockdown would modulate Ataxin-2 cytotoxicity and found that the silencing of Dicer expression only partially impacted cell death in $SCA2_{CAG104}$-expressing cells (Figure 2K). Our data support a role of sCAG RNA in Ataxin-2 cytotoxicity.

We next employed the $SCA2^{\Delta ATG}{}_{CAG115}$ cell model, which only produces sCAG RNA (Figure 2A) and CAG RNA foci (Figure 2D) but not polyQ aggregates (Figure 2D), to examine the cytotoxicity of CAG RNA foci. We found that knock down of Dicer expression abolished sCAG RNA production in $SCA2^{\Delta ATG}{}_{CAG115}$-expressing cells (Figure 2H). By means of *in situ* hybridization, we confirmed that CAG RNA foci formation in these cells was not altered upon Dicer knockdown (Figures 2I and 2J). When compared with the control cells, we continued to detect significant cytotoxicity in the non-translatable $SCA2^{\Delta ATG}{}_{CAG115}$-expressing cells under the Dicer-knockdown condition (Figure 2K). This demonstrates that CAG RNA foci contribute to Ataxin-2 cytotoxicity.

In the $SCA2_{CAA/G104}$-construct-transfected cells, we only detected polyQ protein aggregates (Figure 2D) but not sCAG RNA production (Figure 2A) nor CAG RNA foci formation (Figure 2D). Despite this, we could still detect cytotoxicity in $SCA2_{CAA/G104}$-expressing cells when compared with controls (Figure 2G). This clearly demonstrates that polyQ protein contributes to Ataxin-2 cytotoxicity in our cellular system. Taken together, the above analysis demonstrates that sCAG RNA, CAG RNA foci, and polyQ aggregates all contribute to Ataxin-2 cytotoxicity.

BIND treatment fully rescues neurites and synapse loss in mutant Ataxin-2-expressing mouse primary cortical neurons

After studying the pathogenic deficits at the molecular level, we moved to mouse primary cortical neurons to examine whether neurodegeneration occurred in the form of neurites and synaptic defects upon overexpression of the mutant Ataxin-2 constructs. Immunostaining of neuronal synaptic markers was performed to assess the integrity of neuronal synapses. In *EGFP-*$SCA2_{CAG104}$-expressing neurons, a dramatic reduction in the number of Synapsin I (Figures 3A and 3B), Bassoon (Figures 3C and 3D), and Homer 1 (Figures 3E and 3F) puncta was observed. Synapsin I, as a presynaptic marker, is a neuron-specific phosphoprotein that regulates synaptic vesicle neurotransmitter release.[23] Bassoon is a presynaptic cytomatrix protein responsible for developing presynaptic terminals.[24] Homer 1 is a core scaffold protein that mediates postsynaptic signaling transduction.[25] The sharp drops in these three marker levels (Figures 3A–3F) reflected both pre- and postsynaptic damage to the neurons. Neurite morphologies and arborization were also analyzed. We found that all of the primary (Figure 3G), secondary (Figure 3H), and tertiary (Figure 3I) neurites experienced extensive neurite loss when expressing the *EGFP-*$SCA2_{CAG104}$ construct.

Our group previously reported a peptide inhibitor, BIND, that binds directly to expanded CAG RNA and is capable of alleviating polyQ toxicity both *in vitro* and *in vivo*.[12] In this study, a cell-penetrating peptide, TAT, was linked to the N terminus of BIND to promote cellular delivery of the inhibitor. We next conducted a TAT-BIND treatment assay using *EGFP-*$SCA2_{CAG104}$-transfected neurons to examine whether this expanded CAG RNA binder would rescue neurite loss and synaptic defects. Immunostaining analysis showed that treatment with 10 μM TAT-BIND attained full suppression of the synaptic defects, and synapse integrity was recovered, with significantly elevated expression of all three synaptic markers: Synapsin I (Figures 3J and 3K), Bassoon (Figures 3J and 3L), and Homer 1 (Figures 3J and 3M). Neurite morphology was also restored to the normal level seen in the untransfected or unexpanded *EGFP-*$SCA2_{CAG22}$ controls (Figures 3N–3P). These findings clearly indicate that the expanded CAG RNA inhibitor BIND is capable of rescuing polyQ-induced neurotoxicity.

BIND treatment suppresses mutant Ataxin-2-induced cytotoxicity by simultaneously inhibiting sCAG RNA production, RNA foci formation, and protein aggregation

To further investigate the details of the molecular mechanisms behind the suppression effect of BIND against polyQ-induced cytotoxicity, we next examined whether BIND could alter sCAG RNA production, RNA foci formation, or protein aggregation in our polyQ cell models. BIND was originally discovered as an expanded CAG RNA inhibitor. Thus, we first examined its suppression effect on CAG RNA toxicity in an $EGFP_{CAG78}$-transfected cell model. The expanded CAG-repeat sequences were placed in the untranslated region of the construct to prevent the translation of polyQ protein. We found that TAT-BIND treatment fully suppressed $EGFP_{CAG78}$-induced cell death (Figure S3A) through the inhibition of sCAG RNA production (Figure S3B), DNA damage (Figure S3C), and expanded CAG RNA foci formation (Figures S3D and S3E). We next confirmed the rescuing effect of TAT-BIND in our Ataxin-2 cell model to show that TAT-BIND treatment dose dependently inhibited the cell death induced by $SCA2_{CAG104}$, whereas full suppression was also achieved with 10 μM TAT-BIND treatment (Figure 4A). To determine whether TAT-BIND could alter the transcriptional level of $SCA2_{CAG104}$, we conducted RT-PCR and observed that the $SCA2_{CAG104}$ mRNA levels were not altered by TAT-BIND treatment (Figure 4B). We then examined whether the three expanded CAG RNA-derived neurotoxic molecules (sCAG RNAs, CAG RNA foci, and polyQ aggregates) could be inhibited by TAT-BIND treatment in our Ataxin-2 cell model. RT-PCR analysis showed that TAT-BIND treatment inhibited the production of sCAG RNAs in $SCA2_{CAG104}$-expressing cells in a dose-dependent manner (Figure 4C), which subsequently restored the expression of *NUDT16* (Figure 4C). The elevated levels of the phosphorylated protein kinases in the DNA-damage-response signaling pathways (phosphorylated ATR [p-ATR], p-CHK1, p-ATM, and p-CHK2) were reduced together with the level of cleaved caspase 3, indicating the suppression of cell death (Figure 4C).

To demonstrate that TAT-BIND was indeed delivered into the cells, fluorescein isothiocyanate (FITC)-labeled TAT-BIND was used to perform fluorescence microscopic analysis. Intracellular fluorescence signals of TAT-BIND-FITC were detected (Figure 4D). Furthermore, upon treatment with TAT-BIND-FITC, the microscopically visible

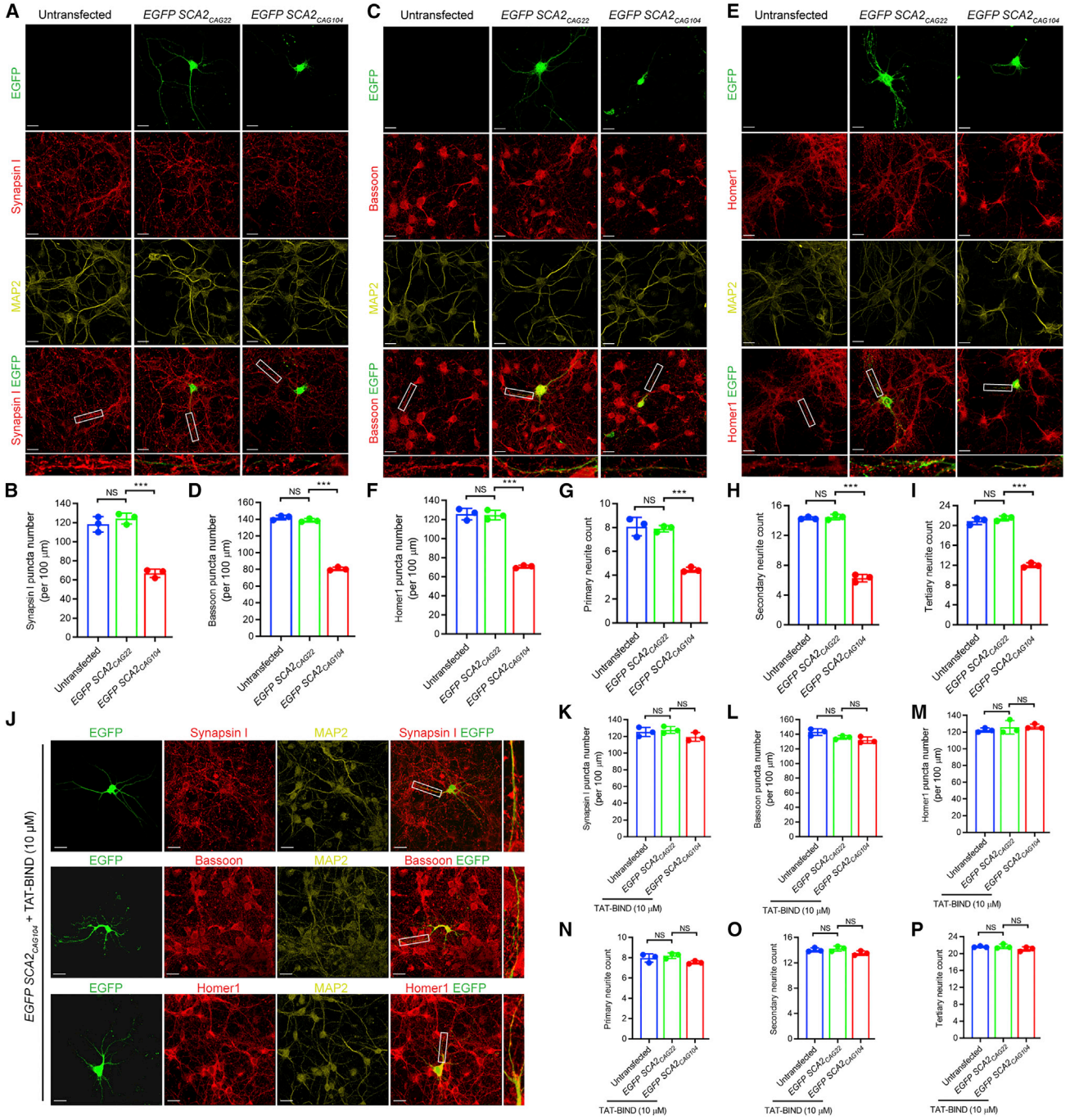

Figure 3. BIND rescues *SCA2$_{CAG104}$*-induced neurites and synapse loss in mouse primary cortical neurons

(A) Representative images of Synapsin I staining of *SCA2$_{CAG104}$*-transfected mouse primary cortical neurons. (B) Quantification of (A). Synapsin I puncta per 100 μm were significantly decreased in *SCA2$_{CAG104}$*-expressing neurons. (C) Representative images of Bassoon staining of mouse primary cortical neurons. (D) Quantification of (C). *SCA2$_{CAG104}$* expression dramatically reduced Bassoon puncta in neurons. (E) Representative images of Homer1 staining of mouse primary cortical neurons. (F) Quantification of (E). Homer1 expression was significantly decreased upon *SCA2$_{CAG104}$* transfection of neurons. (G–I) Primary (G), secondary (H), and tertiary (I) neurites in *SCA2$_{CAG104}$*-transfected neurons were diminished. (J) Representative images of synapsin I, bassoon, and homer1 staining of *SCA2$_{CAG104}$*-expressing neurons upon treatment of BIND. (K–M) Quantification of (J). BIND treatment restored the number of synapsin I, bassoon, and homer1 puncta in *SCA2$_{CAG104}$* neurons. (N–P) The diminished primary (N), secondary (O), and tertiary (P) neurites in *SCA2$_{CAG104}$*-transfected neurons were restored upon BIND treatment. Ten transfected neurons per replica were used for quantification. Scale bars: 20 μm. Error bars represent ± SD. Statistical analysis was performed using one-way ANOVA. NS indicates no significance, ***$p < 0.001$. Experiments were independently repeated for three times. Only representative images are shown.

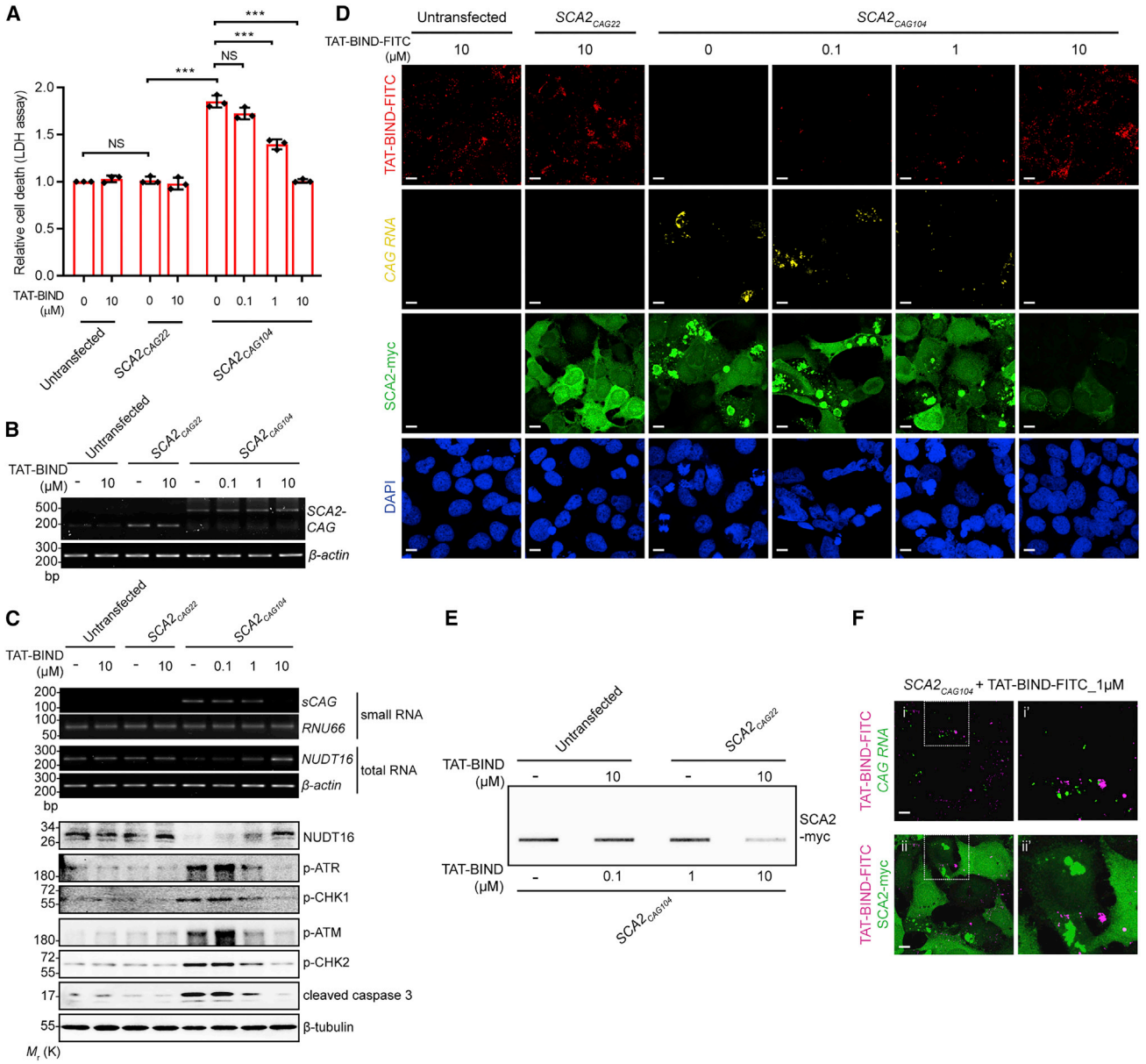

Figure 4. BIND inhibits *sCAG* RNA generation, CAG RNA foci formation, and polyQ protein aggregation in *SCA2$_{CAG104}$*-expressing SK-N-MC cells

(A) BIND treatment rescued *SCA2$_{CAG104}$*-induced cell death in a dose-dependent manner. (B) RT-PCR analysis showed that BIND treatment did not alter the transcript level of *SCA2$_{CAG104}$*. (C) The elevated levels of *sCAG* RNA, p-ATR, p-CHK1, p-ATM, p-CHK2, and cleaved caspase 3 proteins were suppressed upon the treatment of BIND in *SCA2$_{CAG104}$*-expressing SK-N-MC cells. BIND treatment restored NUDT16 at both mRNA and protein levels. (D) Fluorescence microscopic analysis showed that the abundance of both CAG RNA foci and polyQ protein aggregates were reduced upon the treatment of BIND in a dose-dependent manner. (E) Filter-trap assay showed that BIND reduced the level of SDS-insoluble polyQ protein in *SCA2$_{CAG104}$*-expressing SK-N-MC cells. (F) BIND did not co-localize with CAG RNA foci nor polyQ protein aggregates. Scale bars: 10 μm. Error bars represent ± SD. Statistical analysis was performed using one-way ANOVA. NS indicates no significance, ***$p < 0.001$. *RNU66*, *beta-actin*, and beta-tubulin were used as loading controls. Experiments were independently repeated for three times. Only representative images, gels, and blots are shown.

SCA2$_{CAG104}$-induced RNA foci and polyQ aggregates were observed to gradually reduced in a dose-dependent manner (Figure 4D). Additionally, filter-trap analysis verified the dose-dependent decrease in the level of SDS-insoluble polyQ aggregates after treatment (Figure 4E). Our fluorescence microscopic analysis further showed that TAT-BIND-FITC did not co-localize with the CAG RNA foci nor the polyQ aggregates (Figure 4F), indicating that TAT-BIND-FITC does not interact with these toxic species. We further demonstrated that

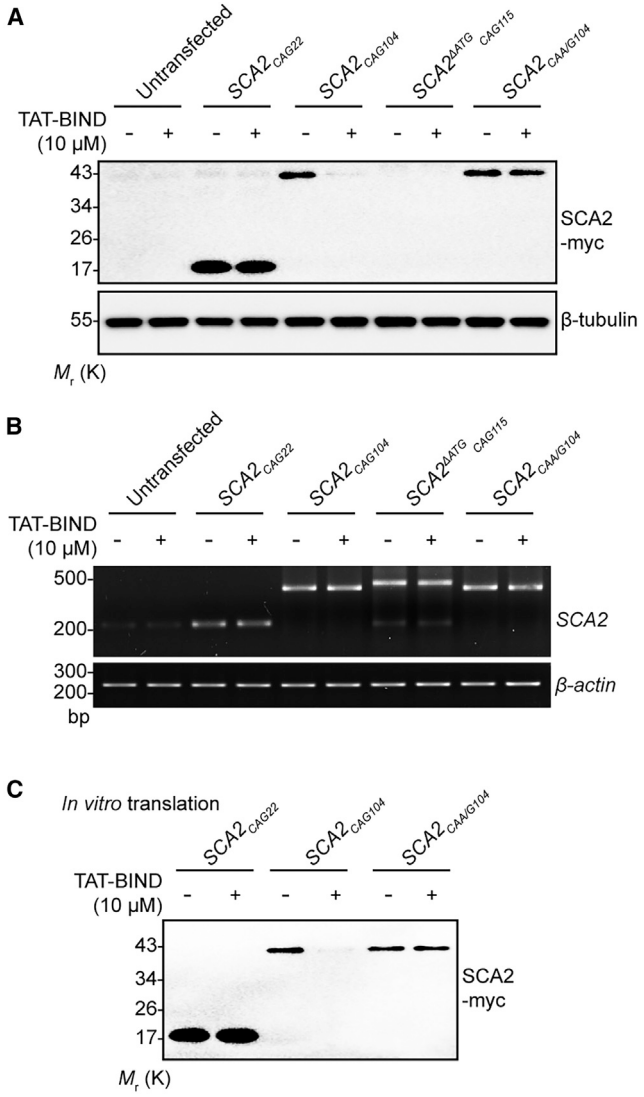

Figure 5. BIND suppresses mutant Ataxin-2 protein translation

(A) BIND treatment reduced the soluble polyQ protein level in $SCA2_{CAG104}$- but not $SCA2_{CAA/G104}$-expressing SK-N-MC cells. (B) Transcriptional levels of *SCA2* were not affected upon the treatment of BIND. (C) *In vitro* protein translation assay demonstrated that BIND treatment inhibited protein translation of $SCA2_{CAG104}$ but not $SCA2_{CAG22}$ and $SCA2_{CAA/G104}$. *Beta-actin* and beta-tubulin were used as loading controls. Experiments were independently repeated for three times. Only representative gels and blots are shown.

TAT-BIND-FITC reduced RNA foci formed by the untranslatable $SCA2^{\Delta ATG}{}_{CAG115}$ transcripts (Figures S4A and S4B). Regarding protein aggregation, polyQ aggregates formed by $SCA2_{CAG104}$ could be suppressed upon the treatment of TAT-BIND-FITC (Figures S4A, S4C, and S4D). In contrast, BIND failed to mitigate protein aggregation in cells transfected with the non-continuous CAG construct $SCA2_{CAA/G104}$. This highlights that CAG continuity in the mutant gene plays a determining role in BIND suppression. These findings are in line with our previous observation that BIND binds expanded CAG RNA.[12]

BIND treatment inhibits mutant Ataxin-2 protein translation

We attempted to further delineate BIND's effect on the suppression of polyQ protein aggregates in $SCA2_{CAG104}$-expressing cells (Figure 4D). We found that BIND treatment only leads to a reduction in the $SCA2_{CAG104}$ protein level (Figure 5A) but not $SCA2_{CAG104}$ transcript level (Figure 5B). Given that we previously demonstrated a direct and physical interaction between BIND and *SCA2* transcripts,[12] we hypothesized that BIND associates with transcribed $SCA2_{CAG104}$ RNA, through which it interferes with SCA2 polyQ protein translation. To test this, we conducted an *in vitro* protein translation assay and found that BIND treatment inhibits protein translation of $SCA2_{CAG104}$ but not unexpanded $SCA2_{CAG22}$ and $SCA2_{CAA/G104}$ which lacks a continuous CAG tract (Figure 5C). Combined with the finding demonstrating that BIND is not capable of suppressing protein aggregation of the non-continuous CAG-repeat $SCA2_{CAA/G104}$ gene product (Figure S4A), our data further support that BIND does not directly act on protein aggregation; instead, it influences protein aggregation indirectly through compromising mutant polyQ protein translation.

BIND treatment suppresses the sequestration of endogenous TDP-43 protein into mutant Ataxin-2 protein aggregates

In 2006, the 43 kDa transactivation response (TAR) DNA-binding protein (TDP-43) was reported as the major disease component in ubiquitinated inclusions in amyotrophic lateral sclerosis (ALS) and frontotemporal lobar degeneration (FTLD).[26] Subsequent studies further highlighted that TDP-43 is susceptible to misfolding, which induces neuronal cytotoxicity, in other neurodegenerative diseases (including polyQ diseases).[27] Interestingly, TDP-43 was shown to be sequestered into polyQ protein aggregates through a Q/N-rich domain at the C terminus.[28] We thus aimed to investigate whether TDP-43 protein would form pathologic aggregates in our Ataxin-2 cell models and whether BIND would inhibit such aggregation. Fluorescence microscopic analysis showed that, along with increased CAG RNA foci and polyQ aggregates, abnormal TDP-43 aggregates were accumulated in $SCA2_{CAG42/72/104}$-expressing cells, and such aggregation was positively correlated with the CAG-repeat lengths of the Ataxin-2 constructs (Figures 6A and 6F). We further found that all of the microscopically visible TDP-43 aggregates were positively stained for mutant Ataxin-2 protein (Figures 6B and 6D). However, we did not find that TDP-43 co-localized with expanded CAG RNA foci (Figures 6B and 6C).

More importantly, TAT-BIND treatment not only reduced polyQ aggregation (Figures S5A–S5D) but also released aggregated TDP-43 (Figures 6E, 6F, and S5A) in $SCA2_{CAG42/72/104}$-transfected cells. Thus, the subsequently enhanced cell death was fully suppressed (Figure S5E). BIND treatment interferes with disease protein translation followed by a reduction in polyQ protein aggregation (Figure 5 and S4). The reduction of soluble mutant Ataxin-2 protein in the $SCA2_{CAG104}$-expressing cells was accompanied with a restoration of soluble TDP-43 protein level (Figure 6G). This highlights a beneficial effect of BIND's action on inhibiting polyQ protein translation.

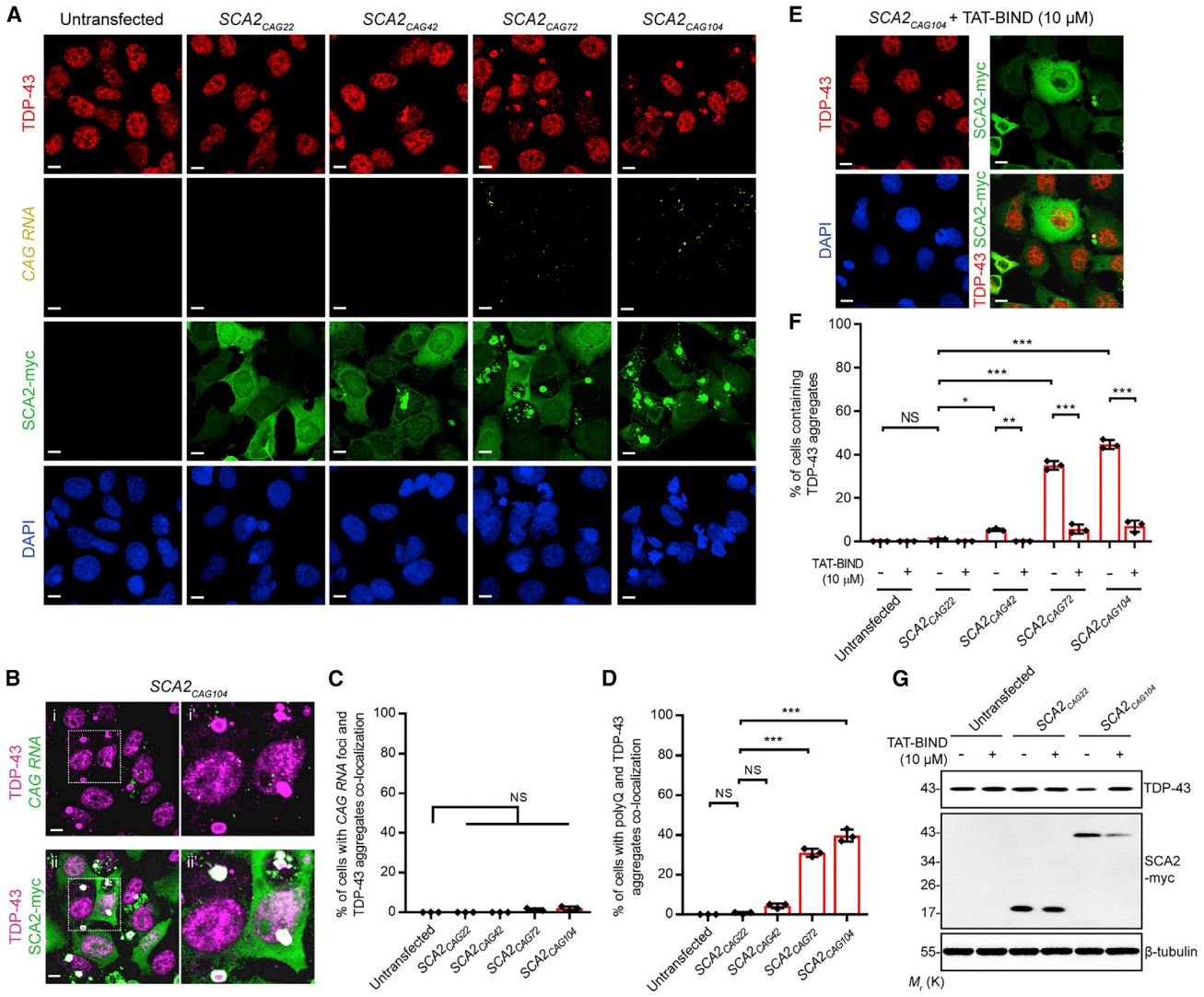

Figure 6. BIND released endogenous TDP-43 protein from Ataxin-2 protein aggregates

(A) The recruitment of TDP-43 protein to Ataxin-2 aggregates was positively correlated with the CAG repeats. (B) Endogenous TDP-43 co-localized with polyQ protein aggregates but not CAG RNA foci. Scale bars: 10 μm. (C and D) Quantification of (B). (E) TDP-43, polyQ protein aggregates, and CAG RNA foci were diminished upon the treatment of BIND in $SCA2_{CAG104}$-expressing SK-N-MC cells. Scale bars: 10 μm. (F) Quantification of (E). (G) Western blot analysis showed that BIND treatment restored the soluble TDP-43 protein level and reduced the soluble polyQ protein in $SCA2_{CAG104}$-expressing SK-N-MC cells. Error bars represent ± SD. Statistical analysis was performed using one-way ANOVA. NS indicates no significance, ***$p < 0.001$. Beta-tubulin was used as loading control. Experiments were independently repeated for three times. Only representative images and blots are shown.

DISCUSSION

Expanded repeat mutant transcripts, mutant proteins, microscopically visible mutant RNA foci, and protein aggregates have been reported to play certain roles in the pathogenesis of repeat expansion diseases.[29,30] Small CAG RNA is produced through the cleavage of elongated mutant CAG transcripts by the endonuclease Dicer.[9,15] The sCAG products trigger gene silencing of CUG-containing transcripts via the RNA-induced silencing complex.[9,10] More than 12,000 human mRNAs carry at least two consecutive CUG triplet repeats.[31] Although not all of these CUG-containing mRNAs are expressed in the nervous system, their numbers highlight that sCAGs produced from mutant CAG transcripts can elicit a spectrum of gene-silencing effects that contribute to neuronal dysfunction and degeneration. Expanded CAG RNA is aggregation prone, and RNA foci formed in cells recruit cellular proteins such as RNA splicing factors,[5,32] leading to spliceopathies. Besides being substrates used for the production of sCAG RNA or taking part in RNA foci formation, intact expanded CAG RNAs that are accessible to the translational machinery produce expanded polyQ protein. Both insoluble and microscopic aggregated forms of mutant polyQ proteins play

principal pathogenic roles in polyQ degeneration.[1] Increasing numbers of polyQ protein species are being identified and assigned to different downstream pathogenic pathways.[33–35] A more thorough understanding of the pathogenic pathways mediated through individual toxic polyQ species will enable us to unravel the most upstream step of pathogenesis and to devise new therapeutic strategies targeting this neurotoxic culprit to treat polyQ degeneration.

In a cell-based model of Ataxin-2, we detected sCAG RNA production, RNA foci formation, and polyQ protein aggregation and further demonstrated that the abundance of these pathological hallmarks correlated with CAG-repeat length and expression time (Figures 1 and S2). Previous investigations also reported that the overexpression of mutant Ataxin-2 induced cell death in a polyQ length- and time-dependent manner.[36] Besides, using $SCA2^{\Delta ATG}{}_{CAG115}$ and $SCA2_{CAA/G104}$ models, we demonstrated that sCAG RNA, CAG RNA foci, and polyQ protein all contribute to mutant Ataxin-2 cytotoxicity (Figure 2). We further observed that mutant Ataxin-2 induced synaptic defects characterized by the reduction of both pre- and postsynaptic components and significant neurite loss in a mouse primary cortical neuron model (Figure 3). This finding is consistent with the spine morphological defects observed in an Ataxin-2 knockin mouse model.[37] Transcribed expanded CAG RNA is the most upstream toxic culprit of these neurotoxic species (sCAG RNA, CAG RNA foci, and polyQ protein aggregates). As such, targeting the CAG RNA to block all of the downstream pathogenic pathways represents a novel therapeutic strategy.

We previously identified a 21 amino acid peptide inhibitor,[12] BIND, that can suppress mutant GGGGCC repeat toxicity, inhibit RNA foci formation, and reduce dipeptide repeat protein production in C9ALS/FTD models.[38] This inhibitor was derived from the wild-type NCL protein sequence and has no cytotoxic effect in primary cortical neurons at a dose of 25 μM.[12] Our earlier work also showed that BIND can rescue the CAG toxicity of polyQ degeneration *in vivo*. Mechanistically, BIND suppresses the nucleolar stress induced by mutant expanded CAG RNA in HEK293 cellular and *Drosophila* polyQ disease models.[12] Given the comprehensive suppression effects of BIND on GGGGCC toxicity, we performed a thorough investigation of its mechanisms of action in polyQ degeneration. Upon treatment with 10 μM TAT-BIND, both neuronal synaptic defects (Figure 3) and cytotoxicity (Figures 4A and 4C) were almost completely ameliorated in both our primary neuron and SK-N-MC Ataxin-2 cell models. Such observations are consistent with our previous findings[12] and further highlight the therapeutic potential of this peptide inhibitor in neurons. Zhang et al.[12] reported that BIND interacts directly with Ataxin-2 CAG RNA and that its binding affinity for CAG RNA is CAG-repeat-length-dependent. Interestingly, we showed that BIND does not alter mutant Ataxin-2 gene transcription (Figure 4B). We further investigated the suppression effects of BIND on three hallmark pathogenic species (sCAG RNA, RNA foci, and polyQ protein aggregates) in our Ataxin-2 cell model. We discovered that sCAG RNA production, mutant Ataxin-2 RNA foci formation, and Ataxin-2 polyQ protein aggregation were diminished (Figures 4C–4E). This finding pinpoints BIND's action on mutant Ataxin-2 transcripts, through which it inhibits Dicer action on sCAG RNA production.[7]

We did not observe co-localization of BIND and CAG RNA foci (Figure 4F). This suggests that BIND does not act by dissolving RNA foci that have already formed. Rather, we argue that BIND interferes with inter-molecular mutant Ataxin-2 RNA association and the interactions of these RNAs with cellular proteins to form RNA foci.[5] When Dicer expression was knocked down in the untranslatable $SCA2^{\Delta ATG}{}_{CAG115}$-expressing cells, we detected only CAG RNA foci (Figure 2I) but not sCAG RNA production (Figure 2H) nor polyQ protein aggregation. Residual cell death was observed in such cells, indicating that CAG RNA foci were cytotoxic (Figure 2K). The inhibitory effect of BIND on CAG RNA foci cytotoxicity can be mediated through its direct physical interaction with expanded SCA2 CAG RNA.[12] It was previously reported that treating Huntington's disease patient fibroblasts with complementary CUG oligonucleotide could reduce RNA foci formation.[39] This argues that the direct physical association of suppression agents, such as the BIND peptide, with mutant CAG RNA transcripts may serve as a physical barrier to interfere with inter-molecular CAG RNA and/or CAG RNA-protein interactions, and as a result, RNA foci formation is inhibited.

We showed that BIND treatment reduces soluble polyQ protein expression in $SCA2_{CAG104}$-expressing cells (Figure 5A) and diminishes polyQ protein aggregation (Figure 4D). In contrast, no such suppression effect was observed in cells transfected with the $SCA2_{CAA/G104}$ construct whose CAG-repeat continuity are interrupted by the alternative glutamine codon CAA (Figures 5A and S4A). In addition, our *in vitro* protein translation analysis demonstrated that BIND treatment only inhibited protein translation of the $SCA2_{CAG104}$ construct but not that of the $SCA2_{CAA/G104}$ construct (Figure 5C). As CAG-repeat continuity is the only difference between the $SCA2_{CAG104}$ and $SCA2_{CAA/G104}$ constructs, this strongly argues that the direct binding of BIND on continuous expanded CAG-repeat RNA in $SCA2_{CAG104}$ mediates protein translation inhibitory of BIND, which leads to the suppression of protein toxicity in the Ataxin-2 cell model.

The BIND sequence does not contain any consecutive glutamine stretches, and it is therefore unlikely that it interacts with polyQ proteins to prevent aggregate formation like previously reported peptide inhibitors.[40,41] Our immunofluorescence results support this line of thought. We did not observe co-localization of BIND with mutant Ataxin-2 protein aggregates (Figure 4F). Taken together, occupying continuous expanded CAG RNA sequences is considered to be a key mechanistic basis for the protective effects of BIND against sCAG RNA, RNA foci, and polyQ protein toxicities of mutant Ataxin-2.

The TDP-43 protein contains two RRMs.[42] Despite its normal cellular roles in RNA metabolism, such as RNA splicing, TDP-43 has been detected in polyQ protein aggregates in patients with polyQ disease,[43]

including those with SCA2.[44] A structural-functional study showed that the glutamine/asparagine-rich region in the C-terminal domain of TDP-43 mediates the sequestration of this protein into polyQ protein aggregates.[28] Consistent with this finding, our immunofluorescence results revealed the co-localization of TDP-43 with mutant Ataxin-2 polyQ protein aggregates (Figures 6B and 6D). Our Ataxin-2 cell model includes both RNA foci and polyQ protein aggregates, allowing us to investigate whether TDP-43 associates with CAG RNA foci. Although TDP-43 contains two RRMs, we did not observe its co-localization with RNA foci (Figures 6B and 6C). This finding suggests that unlike spliceopathies, which are caused by the association of splicing factors such as muscleblind-like 1 with mutant CAG RNA,[29] the sequestration of TDP-43 to polyQ aggregates, but not RNA foci, likely plays a major role in the RNA metabolism defects seen in polyQ pathogenesis.

Importantly, we found that the sequestration of TDP-43 into polyQ aggregates was totally suppressed upon BIND treatment (Figures 6E and 6F). Although only Ataxin-2 protein with intermediate-length polyQ tracts (27–33 Qs) was reported to associate with TDP-43 in patients with ALS,[45] BIND is likely a potent therapeutic candidate for ALS. Further modification of BIND to target intermediate-length CAG RNA should reduce the involvement of Ataxin-2 proteins and lower the risk of developing ALS. The GGGGCC repeat RNA-associated toxicity-alleviating property of BIND[38] also warrants further investigation of its potential in the treatment of ALS and other neurodegenerative diseases.

In summary, the peptide inhibitor BIND targets multiple toxic species in polyQ pathogenesis. BIND does not influence mutant CAG transcript levels (Figure 4B). By directly interacting with mutant CAG transcripts,[12] BIND interferes with sCAG RNA production, CAG RNA foci formation, and polyQ protein translation. Fusing the cell-penetrating peptide TAT[46] to the N terminus of BIND facilitates efficient cellular uptake of BIND.[12] When appended to BIND, the 11 amino acid TAT cell-penetrating peptide sequence increases the molecular size. This modification reduces the chances of the molecule crossing the blood-brain barrier and makes BIND more vulnerable to proteolytic degradation during drug delivery. Further modifications to the N- and C termini of BIND will further improve its stability and ability to enter the brain. For instance, we previously showed that lipidation can be used to replace the TAT sequence to achieve greater stability, cell penetration, and brain uptake of peptide inhibitors.[47]

MATERIALS AND METHODS

Plasmids, siRNAs, and peptides used in this study

The *pEGFP*$_{CAG27/78}$[14] and *pcDNA3.1-SCA2*$_{CAG22/42/72/104}$*-myc*[11] constructs were described previously. To generate the *pSCA2*$_{CAG22/104}$*-EGFP* construct, the *SCA2*$_{CAG22/104}$ DNA fragments were subcloned from *pcDNA3.1-SCA2*$_{CAG22/104}$*-myc* to *pEGFP-N1* (Clontech Laboratories) using *Xho*I and *Hin*dIII. To generate the *pcDNA3.1-SCA2*$^{\Delta ATG}{}_{CAG115}$ and *pcDNA3.1-SCA2*$_{CAA/G104}$*-myc* constructs, the *SCA2*$^{\Delta ATG}{}_{CAG115}$ and *SCA2*$_{CAA/G104}$ DNA fragments were synthesized by GENEWIZ and subcloned into *pcDNA3.1* vector using *Xho*I and *Eco*RI. *Dicer* (L-003483-00) ON-TARGETplus SMARTpool small interfering RNAs (siRNAs) were purchased from Dharmacon, Horizon Discovery. Non-targeting siRNA (D-001210-01-50) was used as control.

TAT-BIND and TAT-BIND-FITC peptides were purchased from GenScript (Piscataway, NJ, USA). Original sequence of BIND was AEIRLVSKDGKSKGIAYIEFK. The TAT cell-penetrating peptide sequence, YGRKKRRQRRR,[48] was attached to the N terminus of BIND. FITC was attached to the C terminus of TAT-BIND for fluorescence detection. All peptides used were high-performance liquid chromatography (HPLC) purified and with a purity over 90%.

Cell culture, transfection, and drug treatment

SK-N-MC cells (American Type Culture Collection [ATCC]) were cultured in DMEM (GE Healthcare BioSciences) supplemented with 10% fetal bovine serum and 1% penicillin–streptomycin. The cells were maintained in a 37°C humidified cell culture incubator supplemented with 5% CO_2. DNA constructs and siRNA were transfected with Lipofectamine 2000 (Thermo Fisher Scientific) and Lipofectamine RNAiMAX (Thermo Fisher Scientific), respectively. After transfection, TAT-BIND or TAT-BIND-FITC peptides were applied with Opti-MEM medium (Thermo Fisher Scientific).

Mouse primary cortical neuron culture, transfection, and drug treatment

Mouse primary cortical neurons were harvested from E16 embryos of C57BL/6J wild-type mouse and cultured as previously described.[10] Briefly, cortical lobes were dissected out in ice-cold PBS glucose. Cortices were digested in trypsin solution after removing the meninges. Primary cortical neurons were cultured on poly-l-lysine-coated (0.05 mg/mL) glass coverslips in 24-well plates (50,000 cells per well). Neurons were maintained in a 37°C humidified cell culture incubator supplemented with 5% CO_2 and were allowed to mature for 5 days before transfection and drug treatment.

Primary neurons were transfected with DNA constructs together with Lipofectamine LTX and Plus Reagent (Thermo Fisher Scientific). Following the manufacturer's protocol of 4 h posttransfection, culture medium was refreshed, and the TAT-BIND peptide of 10 μM was treated. Neurons were further incubated for 48 h to allow recovery and ectopic expression. All animal procedures were approved by the CUHK Animal Experimentation Ethics Committee.

Immunocytochemistry

For immunostaining, neurons were fixed with 4% paraformaldehyde for 10 min at room temperature, followed by permeabilizing with 0.2% Triton X-100 in PBS for 10 min. After permeabilization, neurons were blocked with 1% BSA in PBS for 1 h at room temperature. Primary antibody incubation was performed in 1% BSA overnight at 4°C. After washing with PBS 5 times, samples were incubated with secondary antibodies in 1% BSA in dark for another hour at room temperature. Samples were stained with 1 μg/mL 4,6-diamidino-2-phenylindole (DAPI)

solution for nuclei and then washed with PBS 5 times, followed by mounting and examination under a confocal microscope (Leica TCS SP8 high-speed imaging system with CO_2 incubator). To analyze the neurite arborization and quantify the synaptic markers, primary neurons were stained with MAP2 (1:10,000; ab5392, Abcam) and synapsin I (1:200; ab8, Abcam), Bassoon (1:200; ab82958, Abcam), or Homer1 (1:200; ab97593, Abcam) antibodies. Quantification and statistical analyses were performed on the z stacked maximal projected images by using Photoshop 2020 (Adobe Systems). Only EGFP-positive neurons were used for the statistical analysis. Ten transfected neurons per replicate were used in the analysis.

FISH

Cells were fixed with 4% paraformaldehyde/DEPC-PBS for 15 min and permeabilized with 0.2% Triton X-100/DEPC-PBS for 10 min at room temperature. Samples were washed with DEPC-PBS twice and hybridized with 30 nM denatured TYE563-labeled Affinity Plus DNA probe (5′-TYE563-C+TGC+TGC+TGCTG+CTG+CTG+CT-3'; Integrated DNA Technologies)[49] in hybridization buffer (50% formamide, 10% dextran sulfate, 2× saline-sodium citrate (SSC) and 50 mM sodium phosphate buffer) for 4 h at 65°C. After hybridization, cells were washed with 2× SSC/0.1% Tween-20 buffer 3 times at 65°C, followed by further washing with 0.1× SSC buffer 3 times at 65°C. Cells were then blocked with 1% BSA in DEPC-PBS for 1 h at room temperature and stained with anti-myc (1:200; 2276, CST) and anti-TDP-43 (1:100; ab109535, Abcam) overnight at 4°C. After washing with DEPC-PBS 5 times, cells were incubated with secondary antibodies in dark for 1 h at room temperature. Nuclei were counterstained with DAPI solution prior to mounting on cover slips. Images were obtained using a Leica TCS SP8 confocal microscope.

RNA extraction and RT-PCR

Total cellular RNA was isolated from SK-N-MC cells using TRIzol reagent (Thermo Fisher Scientific), followed by RT using the ImProm-IITM Reverse Transcription System (Promega) according to the manufacturer's instructions. RNeasy Mini Kit (Qiagen) and RNeasy MinElute Cleanup Kit (Qiagen) were used for the purification of small RNA species following the manufacturer's instructions. After purification, enriched small RNAs were then polyadenylated using poly(A) polymerase (Ambion) in the presence of $MnCl_2$ (2.5 mM) and ATP (1 mM) for 1 h at 37°C. polyA-tailed small RNAs were then annealed with a polyT-enriched RT adapter (5′-CGAATTCTAGAGCTCGAGGCAGGCGACATGGCTGGCTAGTTAAGCTTGGTACCGAGCTCGGATCCACTAGTCCTTTTTTTTTTTTTTTTTTTTTTTAC-3′), followed by the RT reaction.[9] Primers used in this study were *sCAG*-F, 5′-CAGCAGCAGCAGCAGCAG-3′; *sCAG*-R, 5′-CGAATTCTAGAGCTCGAGGCAGG-3′; *RNU66*-F, 5′-GTAACTGTGGTGATGGAAATGTG-3′; *RNU66*-R, 5′-GACTGTACTAGGATAGAAAGAACC-3′; *NUDT16*-F, 5′-CTGCGCTACGCCATACTGAT-3′; *NUDT16*-R, 5′-GTCAGACGCTTGGCATAGAAG-3′; *SCA2-CAG*-F, 5′-CTCACCATGTCGCTGAAG-3′; *SCA2-CAG*-R, 5′-CGAGGACGAGGAGACC-3′; $CAG_{27/78}$-F, 5′-AAAAACAGCAGCAAAAGC-3′; $CAG_{27/78}$-R, 5′-TCTGTCCTGATAGGTCC-3′; *β-actin*-F, 5′-ATGTGCAAGGCCGGTTTCGC-3′; *β-actin*-R, 5′-CGACACGCAGCTCATTGTAG-3′.

Protein sample preparation, western blotting, and antibodies used in this study

Proteins were extracted from SK-N-MC cells using SDS sample buffer and boiled at 99°C for 10 min prior to western blotting. Primary antibodies used were anti-NUDT16 (SAB2107004, 1:2,000) from Sigma-Aldrich; anti-p-ATR (2853, 1:1,000), anti-p-ATM (5883, 1:1,000), anti-p-CHK1 (2348, 1:1,000), anti-p-CHK2 (2197, 1:1,000), anti-cleaved caspase 3 (9664, 1:500), and anti-myc (2276, 1:2,000) from Cell Signaling Technology; anti-Dicer (ab14601, 1:2,000), anti-TDP-43 (ab109535, 1:2,000), and anti-β-tubulin (ab6046, 1:2,000) from Abcam; and anti-GFP (JL-8, 1:4,000) from Clontech. Secondary antibodies were goat anti-rabbit (11-035-045, 1:5,000) and goat anti-mouse (115-035-062, 1:5,000) from Jackson ImmunoResearch.

Filter-trap assay

Cells were lysed in 2% SDS solution and diluted to a final volume of 200 μL. Protein samples were then loaded to a 48-well Bio-Dot microfiltration apparatus and filtered with cellulose acetate membrane (pore size = 0.2 μm; Sartorius Stedim Biotech, Goettingen, Germany). The membrane was then blocked with 5% non-fat milk prior to primary antibody incubation (anti-myc, same condition used for western blotting) for aggregated protein examination.

In vitro protein translation assay

The *in vitro* protein translation assay was performed using 1-step human coupled IVT kit (Thermo Fisher Scientific) according to the manufacturer's instructions. In each reaction, 4 μg DNA template was used, and the reaction was incubated for 6 h at 30°C. The *in-vitro*-translated protein was then subjected to western blotting for evaluation of the protein expression level.

Comet assay

Single-cell nuclear DNA damage were evaluated using Comet assay Kit (Trevigen) under alkaline condition, following the manufacturer's instructions. Comet images were captured using a Nikon DS-Ri2 camera attached on a BX51 fluorescence microscope. For image analysis and quantification, 100 cells per replicate were analyzed using Open Comet and Image J software.

Lactate dehydrogenase (LDH) assay

Upon cytotoxic insults, eukaryotic cellular membrane may damage and release the cytosolic LDH to cell culture medium. The enzyme activity has been shown to be directly proportional to cell death. The LDH assay is a standard colorimetric quantitative assay to measure the enzyme activity.[50] The LDH assay on SK-N-MC cells were performed according to manufacturer's instructions (CytoTox 96 Non-Radioactive Cytotoxicity Assay Kit, Promega).

Statistical analyses

Differences between each group were determined using one-way ANOVA followed by post hoc Tukey's test. NS denotes not

significant. *p < 0.05, **p < 0.01, and ***p < 0.001, which are considered statistically significant.

Data availability statement

All study data are included in the article and/or supplemental information.

SUPPLEMENTAL INFORMATION

Supplemental information can be found online at https://doi.org/10.1016/j.omtn.2022.06.004.

ACKNOWLEDGMENTS

This work was supported by the Research Grants Council General Research Fund (project nos. 14107118 and 14122019); The Chinese University of Hong Kong Vice-Chancellor's One-Off Discretionary Fund (project nos. 4930713 and VCF2014011); Lui Che Woo Institute of Innovative Medicine Brain Research and Innovative Neuroscience Initiative (project no. 8303404); Gerald Choa Neuroscience Centre (project no. 7105306); and Faculty of Medicine, The Chinese University of Hong Kong. Z.S.C. was supported by a Postdoctoral Fellowship in Clinical Neurosciences program between The Chinese University of Hong Kong and University of Oxford (Nuffield Department of Clinical Neurosciences and Pembroke College).

AUTHOR CONTRIBUTIONS

S.I.P. and H.Y.E.C. designed research; S.I.P., J.K.-L.S., and Z.S.C. performed research; S.I.P., L.I.L., H.-M.C., and H.Y.E.C. analyzed data; S.I.P., L.I.L., and H.Y.E.C. wrote the paper.

DECLARATION OF INTERESTS

The authors declare no competing interests.

REFERENCES

1. Lieberman, A.P., Shakkottai, V.G., and Albin, R.L. (2019). Polyglutamine repeats in neurodegenerative diseases. Annu. Rev. Pathol. *14*, 1–27. https://doi.org/10.1146/annurev-pathmechdis-012418-012857.

2. Ordway, J.M., Tallaksen-Greene, S., Gutekunst, C.A., Bernstein, E.M., Cearley, J.A., Wiener, H.W., Dure, L.S., Lindsey, R., Hersch, S.M., Jope, R.S., et al. (1997). Ectopically expressed CAG repeats cause intranuclear inclusions and a progressive late onset neurological phenotype in the mouse. Cell *91*, 753–763. https://doi.org/10.1016/s0092-8674(00)80464-x.

3. McCampbell, A., Taylor, J.P., Taye, A.A., Robitschek, J., Li, M., Walcott, J., Merry, D., Chai, Y., Paulson, H., Sobue, G., et al. (2000). CREB-binding protein sequestration by expanded polyglutamine. Hum. Mol. Genet. *9*, 2197–2202. https://doi.org/10.1093/hmg/9.14.2197.

4. Yamamoto, A., Lucas, J.J., and Hen, R. (2000). Reversal of neuropathology and motor dysfunction in a conditional model of Huntington's disease. Cell *101*, 57–66. https://doi.org/10.1016/s0092-8674(00)80623-6.

5. de Mezer, M., Wojciechowska, M., Napierala, M., Sobczak, K., and Krzyzosiak, W.J. (2011). Mutant CAG repeats of Huntingtin transcript fold into hairpins, form nuclear foci and are targets for RNA interference. Nucleic Acids Res. *39*, 3852–3863. https://doi.org/10.1093/nar/gkq1323.

6. Li, L.B., Yu, Z., Teng, X., and Bonini, N.M. (2008). RNA toxicity is a component of ataxin-3 degeneration in Drosophila. Nature *453*, 1107–1111. https://doi.org/10.1038/nature06909.

7. Krol, J., Fiszer, A., Mykowska, A., Sobczak, K., de Mezer, M., and Krzyzosiak, W.J. (2007). Ribonuclease dicer cleaves triplet repeat hairpins into shorter repeats that silence specific targets. Mol. Cell *25*, 575–586. https://doi.org/10.1016/j.molcel.2007.01.031.

8. Rué, L., Bañez-Coronel, M., Creus-Muncunill, J., Giralt, A., Alcalá-Vida, R., Mentxaka, G., Kagerbauer, B., Zomeño-Abellán, M.T., Aranda, Z., Venturi, V., et al. (2016). Targeting CAG repeat RNAs reduces Huntington's disease phenotype independently of huntingtin levels. J. Clin. Invest. *126*, 4319–4330. https://doi.org/10.1172/jci83185.

9. Bañez-Coronel, M., Porta, S., Kagerbauer, B., Mateu-Huertas, E., Pantano, L., Ferrer, I., Guzmán, M., Estivill, X., and Martí, E. (2012). A pathogenic mechanism in Huntington's disease involves small CAG-repeated RNAs with neurotoxic activity. PLoS Genet. *8*, e1002481. https://doi.org/10.1371/journal.pgen.1002481.

10. Peng, S., Guo, P., Lin, X., An, Y., Sze, K.H., Lau, M.H.Y., Chen, Z.S., Wang, Q., Li, W., Sun, J.K.L., et al. (2021). CAG RNAs induce DNA damage and apoptosis by silencing NUDT16 expression in polyglutamine degeneration. Proc. Natl. Acad. Sci. USA *118*. e2022940118. https://doi.org/10.1073/pnas.2022940118.

11. Zhang, Q., Tsoi, H., Peng, S., Li, P.P., Lau, K.-F., Rudnicki, D.D., Ngo, J.C.-K., and Chan, H.Y.E. (2016). Assessing a peptidylic inhibitor-based therapeutic approach that simultaneously suppresses polyglutamine RNA- and protein-mediated toxicities in patient cells and Drosophila. Dis. Model Mech. *9*, 321–334. https://doi.org/10.1242/dmm.022350.

12. Zhang, Q., Chen, Z.S., An, Y., Liu, H., Hou, Y., Li, W., Lau, K.F., Koon, A.C., Ngo, J.C.K., and Chan, H.Y.E. (2018). A peptidylic inhibitor for neutralizing expanded CAG RNA-induced nucleolar stress in polyglutamine diseases. RNA *24*, 486–498. https://doi.org/10.1261/rna.062703.117.

13. Ginisty, H., Sicard, H., Roger, B., and Bouvet, P. (1999). Structure and functions of nucleolin. J. Cell Sci. *112*, 761–772.

14. Tsoi, H., Lau, T.C.-K., Tsang, S.-Y., Lau, K.-F., and Chan, H.Y.E. (2012). CAG expansion induces nucleolar stress in polyglutamine diseases. Proc. Natl. Acad. Sci. USA *109*, 13428–13433. https://doi.org/10.1073/pnas.1204089109.

15. Krol, J., Fiszer, A., Mykowska, A., Sobczak, K., de Mezer, M., and Krzyzosiak, W.J. (2007). Ribonuclease dicer cleaves triplet repeat hairpins into shorter repeats that silence specific targets. Mol. Cell *25*, 575–586. https://doi.org/10.1016/j.molcel.2007.01.031.

16. Marechal, A., and Zou, L. (2013). DNA damage sensing by the ATM and ATR kinases. Cold Spring Harb. Perspect. Biol. *5*, a012716. https://doi.org/10.1101/cshperspect.a012716.

17. Blackford, A.N., and Jackson, S.P. (2017). ATM, ATR, and DNA-PK: the trinity at the heart of the DNA damage response. Mol. Cell *66*, 801–817. https://doi.org/10.1016/j.molcel.2017.05.015.

18. Kumaravel, T.S., Vilhar, B., Faux, S.P., and Jha, A.N. (2009). Comet Assay measurements: a perspective. Cell Biol. Toxicol. *25*, 53–64. https://doi.org/10.1007/s10565-007-9043-9.

19. Chan, H.Y.E. (2014). RNA-mediated pathogenic mechanisms in polyglutamine diseases and amyotrophic lateral sclerosis. Front. Cell. Neurosci. *8*, 431. https://doi.org/10.3389/fncel.2014.00431.

20. Takeuchi, T., and Nagai, Y. (2017). Protein misfolding and aggregation as a therapeutic target for polyglutamine diseases. Brain Sci. *7*, 128. https://doi.org/10.3390/brainsci7100128.

21. Nalavade, R., Griesche, N., Ryan, D.P., Hildebrand, S., and Krauß, S. (2013). Mechanisms of RNA-induced toxicity in CAG repeat disorders. Cell Death Dis. *4*, e752. https://doi.org/10.1038/cddis.2013.276.

22. Hands, S.L., and Wyttenbach, A. (2010). Neurotoxic protein oligomerisation associated with polyglutamine diseases. Acta Neuropathol. *120*, 419–437. https://doi.org/10.1007/s00401-010-0703-0.

23. Thiel, G. (1993). Synapsin I, synapsin II, and synaptophysin: marker proteins of synaptic vesicles. Brain Pathol. *3*, 87–95. https://doi.org/10.1111/j.1750-3639.1993.tb00729.x.

24. Zhai, R.G., Vardinon-Friedman, H., Cases-Langhoff, C., Becker, B., Gundelfinger, E.D., Ziv, N.E., and Garner, C.C. (2001). Assembling the presynaptic active zone: a characterization of an active zone precursor vesicle. Neuron *29*, 131–143. https://doi.org/10.1016/s0896-6273(01)00185-4.

25. Luo, P., Li, X., Fei, Z., and Poon, W. (2012). Scaffold protein Homer 1: implications for neurological diseases. Neurochem. Int. *61*, 731–738. https://doi.org/10.1016/j.neuint.2012.06.014.

26. Neumann, M., Sampathu, D.M., Kwong, L.K., Truax, A.C., Micsenyi, M.C., Chou, T.T., Bruce, J., Schuck, T., Grossman, M., Clark, C.M., et al. (2006). Ubiquitinated TDP-43 in frontotemporal lobar degeneration and amyotrophic lateral sclerosis. Science *314*, 130–133. https://doi.org/10.1126/science.1134108.

27. Toyoshima, Y., and Takahashi, H. (2014). TDP-43 pathology in polyglutamine diseases: with reference to amyotrphic lateral sclerosis. Neuropathology *34*, 77–82. https://doi.org/10.1111/neup.12053.

28. Fuentealba, R.A., Udan, M., Bell, S., Wegorzewska, I., Shao, J., Diamond, M.I., Weihl, C.C., and Baloh, R.H. (2010). Interaction with polyglutamine aggregates reveals a Q/N-rich domain in TDP-43. J. Biol. Chem. *285*, 26304–26314. https://doi.org/10.1074/jbc.m110.125039.

29. Martí, E. (2016). RNA toxicity induced by expanded CAG repeats in Huntington's disease. Brain Pathol. *26*, 779–786. https://doi.org/10.1111/bpa.12427.

30. Malik, I., Kelley, C.P., Wang, E.T., and Todd, P.K. (2021). Molecular mechanisms underlying nucleotide repeat expansion disorders. Nat. Rev. Mol. Cell Biol. *22*, 589–607. https://doi.org/10.1038/s41580-021-00382-6.

31. Tian, B., Mukhopadhyay, R., and Mathews, M.B. (2005). Polymorphic CUG repeats in human mRNAs and their effects on gene expression. RNA Biol. *2*, 149–156. https://doi.org/10.4161/rna.2.4.2446.

32. Jain, A., and Vale, R.D. (2017). RNA phase transitions in repeat expansion disorders. Nature *546*, 243–247. https://doi.org/10.1038/nature22386.

33. Wong, S.L.A., Chan, W.M., and Chan, H.Y.E. (2008). Sodium dodecyl sulfate-insoluble oligomers are involved in polyglutamine degeneration. FASEB. J. *22*, 3348–3357. https://doi.org/10.1096/fj.07-103887.

34. Berger, T.R., Montie, H.L., Jain, P., Legleiter, J., and Merry, D.E. (2015). Identification of novel polyglutamine-expanded aggregation species in spinal and bulbar muscular atrophy. Brain Res. *1628*, 254–264. https://doi.org/10.1016/j.brainres.2015.09.033.

35. Kim, Y.E., Hosp, F., Frottin, F., Ge, H., Mann, M., Hayer-Hartl, M., and Hartl, F.U. (2016). Soluble oligomers of PolyQ-expanded huntingtin target a multiplicity of key cellular factors. Mol. Cell *63*, 951–964. https://doi.org/10.1016/j.molcel.2016.07.022.

36. Huynh, D.P., Yang, H.-T., Vakharia, H., Nguyen, D., and Pulst, S.M. (2003). Expansion of the polyQ repeat in ataxin-2 alters its Golgi localization, disrupts the Golgi complex and causes cell death. Hum. Mol. Genet. *12*, 1485–1496. https://doi.org/10.1093/hmg/ddg175.

37. Arsović, A., Halbach, M.V., Canet-Pons, J., Esen-Sehir, D., Döring, C., Freudenberg, F., Czechowska, N., Seidel, K., Baader, S.L., Gispert, S., et al. (2020). Mouse ataxin-2 expansion downregulates CamKII and other calcium signaling factors, impairing granule-purkinje neuron synaptic strength. Int. J. Mol. Sci. *21*, 6673. https://doi.org/10.3390/ijms21186673.

38. Zhang, Q., An, Y., Chen, Z.S., Koon, A.C., Lau, K.-F., Ngo, J.C.K., and Chan, H.Y.E. (2019). A peptidylic inhibitor for neutralizing (GGGGCC)-Associated neurodegeneration in C9ALS-FTD. Mol. Ther. Nucleic Acids *16*, 172–185. https://doi.org/10.1016/j.omtn.2019.02.015.

39. Urbanek, M.O., Fiszer, A., and Krzyzosiak, W.J. (2017). Reduction of Huntington's disease RNA foci by CAG repeat-targeting reagents. Front. Cell. Neurosci. *11*, 82. https://doi.org/10.3389/fncel.2017.00082.

40. Nagai, Y., Tucker, T., Ren, H., Kenan, D.J., Henderson, B.S., Keene, J.D., Strittmatter, W.J., and Burke, J.R. (2000). Inhibition of polyglutamine protein aggregation and cell death by novel peptides identified by phage display screening. J. Biol. Chem. *275*, 10437–10442. https://doi.org/10.1074/jbc.275.14.10437.

41. Kazantsev, A., Walker, H.A., Slepko, N., Bear, J.E., Preisinger, E., Steffan, J.S., Zhu, Y.Z., Gertler, F.B., Housman, D.E., Marsh, J.L., and Thompson, L.M. (2002). A bivalent Huntingtin binding peptide suppresses polyglutamine aggregation and pathogenesis in Drosophila. Nat. Genet. *30*, 367–376. https://doi.org/10.1038/ng864.

42. Loughlin, F.E., and Wilce, J.A. (2019). TDP-43 and FUS-structural insights into RNA recognition and self-association. Curr. Opin. Struct. Biol. *59*, 134–142. https://doi.org/10.1016/j.sbi.2019.07.012.

43. Schwab, C., Arai, T., Hasegawa, M., Yu, S., and McGeer, P.L. (2008). Colocalization of transactivation-responsive DNA-binding protein 43 and huntingtin in inclusions of Huntington disease. J. Neuropathol. Exp. Neurol. *67*, 1159–1165. https://doi.org/10.1097/nen.0b013e31818e8951.

44. Toyoshima, Y., Tanaka, H., Shimohata, M., Kimura, K., Morita, T., Kakita, A., and Takahashi, H. (2011). Spinocerebellar ataxia type 2 (SCA2) is associated with TDP-43 pathology. Acta Neuropathol. *122*, 375–378. https://doi.org/10.1007/s00401-011-0862-7.

45. Elden, A.C., Kim, H.J., Hart, M.P., Chen-Plotkin, A.S., Johnson, B.S., Fang, X., Armakola, M., Geser, F., Greene, R., Lu, M.M., et al. (2010). Ataxin-2 intermediate-length polyglutamine expansions are associated with increased risk for ALS. Nature *466*, 1069–1075. https://doi.org/10.1038/nature09320.

46. Rizzuti, M., Nizzardo, M., Zanetta, C., Ramirez, A., and Corti, S. (2015). Therapeutic applications of the cell-penetrating HIV-1 Tat peptide. Drug Discov. Today *20*, 76–85. https://doi.org/10.1016/j.drudis.2014.09.017.

47. Zhang, Q., Yang, M., Sørensen, K.K., Madsen, C.S., Boesen, J.T., An, Y., Peng, S.H., Wei, Y., Wang, Q., Jensen, K.J., et al. (2017). A brain-targeting lipidated peptide for neutralizing RNA-mediated toxicity in Polyglutamine Diseases. Sci. Rep. *7*, 12077. https://doi.org/10.1038/s41598-017-11695-y.

48. Popiel, H.A., Nagai, Y., Fujikake, N., and Toda, T. (2007). Protein transduction domain-mediated delivery of QBP1 suppresses polyglutamine-induced neurodegeneration *in vivo*. Mol. Ther. *15*, 303–309. https://doi.org/10.1038/sj.mt.6300045.

49. Urbanek, M.O., and Krzyzosiak, W.J. (2016). RNA FISH for detecting expanded repeats in human diseases. Methods *98*, 115–123. https://doi.org/10.1016/j.ymeth.2015.11.017.

50. Kumar, P., Nagarajan, A., and Uchil, P.D. (2018). Analysis of cell viability by the lactate dehydrogenase assay. Cold Spring Harb. Protoc. *2018*. pdb.prot095497. https://doi.org/10.1101/pdb.prot095497.